

Supporting information

Origins of High Electrolyte-Electrode Interfacial Resistances in Lithium Cells

Containing Garnet Type LLZO Solid Electrolytes

Lei Cheng,^{1,2} Ethan J. Crumlin,³ Wei Chen,¹ Ruimin Qiao,³ Huaming Hou,^{1,4} Simon Franz Lux,¹ Vassilia Zorba,¹ Richard Russo,¹ Robert Koskecki,¹ Zhi Liu,³ Kristin Persson,¹ Wanli Yang,³ Jordi Cabana,^{1,5} Thomas Richardson,¹ Guoying Chen,¹ and Marca Doeff¹

1. Lawrence Berkeley National Laboratory, Environmental Energy Technologies

Division, University of California, Berkeley, CA 94720, USA

2. Department of Material Sciences and Engineering, University of California, Berkeley,

CA 94720, USA

3. Advanced Light Source, Lawrence Berkeley National Laboratory, University of

California, Berkeley, CA 94720, USA

4. Optics and Optoelectronics Laboratory, Ocean University of China, Qingdao 266100,

China

5. Department of Chemistry, University of Illinois at Chicago, Chicago, IL 60607, USA

Computational

First-principles total energy calculations were carried out using density functional theory and the projector augmented-wave (PAW) approach as implemented in the Vienna ab initio simulation package (VASP)^{1, 2}. The generalized gradient approximation (GGA) of Perdew-Burke-Ernzerhof (PBE) was used to approximate the electronic change and correlation.³ The original structure for LLZO was taken from the Inorganic Crystal Structure Database (ICSD) (Collection code: 422259).⁴ The Li atoms were ordered in a supercell using the Python Materials Genomics (pymatgen) code^{5, 6} with experimental site occupancies reported from ICSD. The cubic structure for $\text{Li}_7\text{La}_3\text{Zr}_2\text{O}_{12}$ was shown in Figure S6, which had 192 atoms (Li 56, La 24, Zr 16 and O 96). All configurations were enumerated so that 2 Li atoms and 1 O atom were removed from the starting LLZO structure. The lowest electrostatic energy configuration was chosen for the LLZO structure after reaction (denoted as $\text{Li}_{54}\text{La}_{24}\text{Zr}_{16}\text{O}_{55}$). These structures were fully relaxed to converge the final energy within 5 meV per formula unit. The plane wave energy cutoff was 520 eV and the Brillouin-zone was sampled at the Γ -point.

The total energies for Li_2O , Li_2CO_3 and LiOH were taken from the Materials Project⁷. These calculations were performed using a compatible set of parameters with the calculations in the current study. The calculated formation enthalpies for all compounds were referenced using a thermodynamic framework that corrects the DFT errors in gases and aqueous states.⁸ In Table S2, we list the calculated formation enthalpies for these Li compounds together with their experimental standard Gibbs free energies. We used the experimental Gibbs free energies for the gas phase H_2O and CO_2 in following thermodynamic calculations.⁹

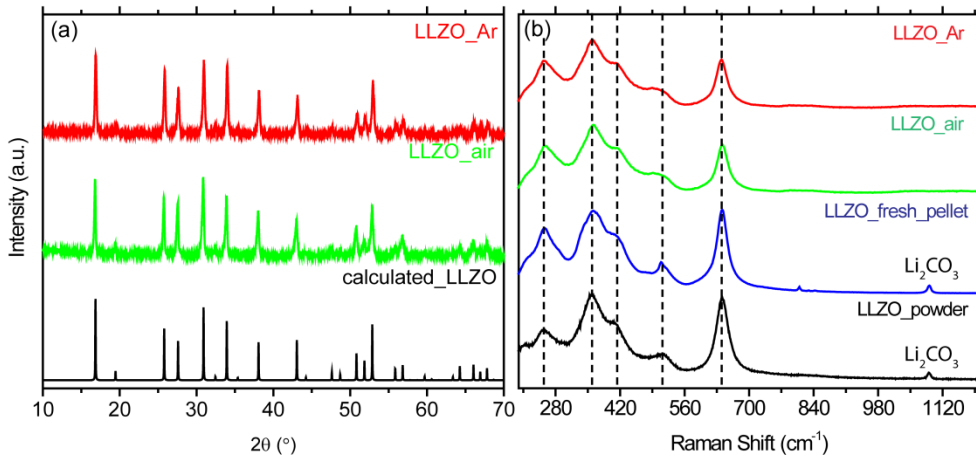


Figure S1 (a) XRD patterns of LLZO_Ar (top), LLZO_air (middle) and a simulated cubic LLZO pattern (bottom) based on reference.¹⁰ (b) Raman spectra of LLZO_Ar (top), LLZO_air (second from top), unpolished LLZO_fresh pellet (second from bottom), and the as-synthesized powder (bottom).

X-ray diffraction (XRD) and Raman spectroscopy were used to obtain further information about the lithium-rich layer on the pellet surface. Figure S1(a) shows the XRD patterns of the LLZO_Ar and LLZO_air samples, which were both consistent with pure cubic LLZO having a lattice parameter of 12.962 \AA . No Li_2CO_3 was detected, but XRD is insensitive to low levels of impurities, particularly those containing light elements. The Raman spectra of as-synthesized powder, the fresh pellet, and polished LLZO_Ar and LLZO_air pellets are shown in Figure S2(b). The estimated penetration depth of the laser used for the Raman experiment is on the order of a few μm , based on the wavelength used, and the fact that LLZO is a whitish electronically insulating material. The results agree very well with spectra reported elsewhere.¹¹ Peaks above 550 cm^{-1} were assigned to vibrational stretching of ZrO_6 units and those between 300 cm^{-1} and 550 cm^{-1} associated with their vibrational bending.¹¹ No apparent differences among the spectra of the different samples were observed in these regions, suggesting that the polishing procedures

did not affect the structure of the main phase. However, a small peak at 1100 cm^{-1} , attributable to Li_2CO_3 , was observed in both the powder and in the fresh pellet, which was absent in the polished pellets.¹² The composition of the LLZO pellet was determined to be $\text{Li}_{5.92}\text{Al}_{0.36}\text{La}_3\text{Zr}_{2.00}\text{O}_{12}$ (data normalized to La) by ICP-OES. Note that the O content was estimated by balancing the charge.

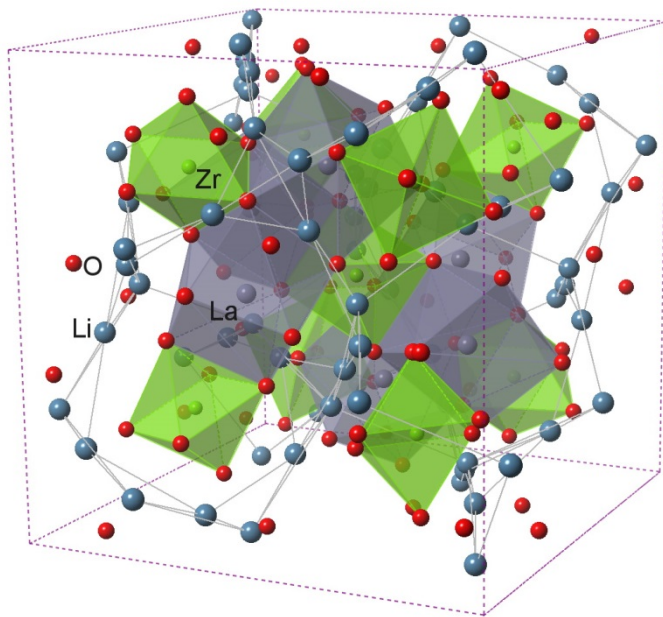


Figure S2, The 192-atom supercell of LLZO used in first-principles calculations.

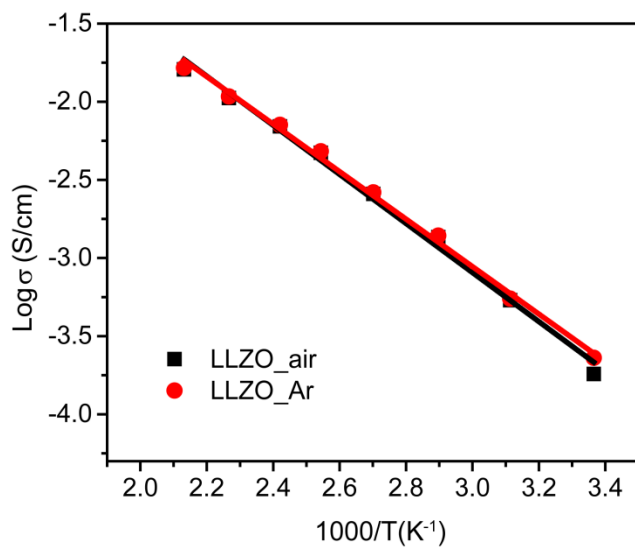


Figure S3. Total ionic conductivities of pellets polished in ambient air (LLZO_air) and in Ar (LLZO_Ar), measured in cells with ion-blocking Au electrodes.

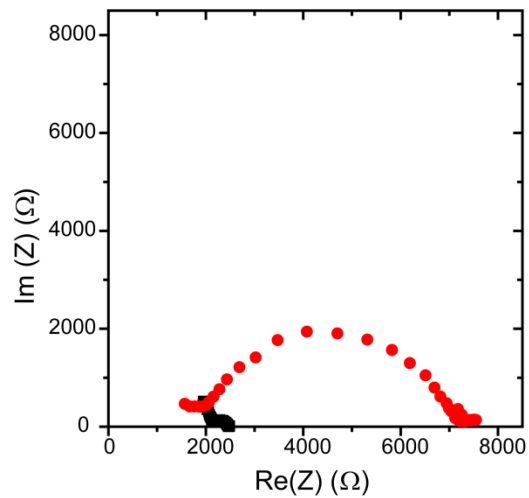


Figure S4. Nyquist plots of Li/LLZO_Ar/Li cells before and after exposure of the LLZO to air and water.

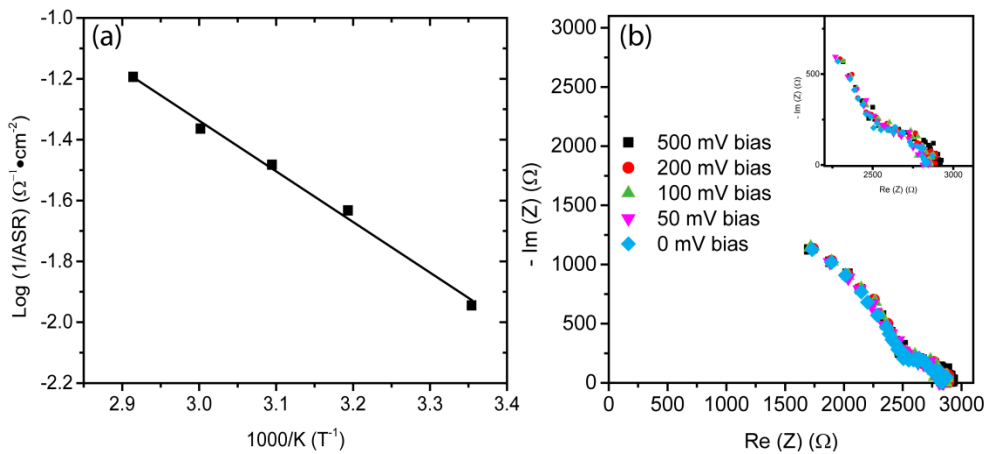


Figure S5. (a) Reciprocal area specific resistance as a function of temperature (b) Nyquist plots of Li/LLZO_Ar/Li cells at varying DC biases.

	Experimental Gibbs free energy $\mu^{0,\text{exp}}$ (eV/fu)	Calculated Gibbs free energy $\mu^{0,\text{DFT}}$ (eV/fu)
Li_2CO_3	-12.60	-12.55
Li_2O	-6.20	-5.87
LiOH	-5.03	-4.69
$\text{Li}_{56}\text{La}_{24}\text{Zr}_{16}\text{O}_{96}$	-	-77.51
$\text{Li}_{54}\text{La}_{24}\text{Zr}_{16}\text{O}_{95}$	-	-71.05
$\text{H}_2\text{O}(\text{g})$	-2.37	-
$\text{CO}_2(\text{g})$	-4.09	-

Table S1 Calculated enthalpies and experimental standard Gibbs free energies⁹ for the compounds used in thermodynamic calculations.

References

1. H. J. Monkhorst and J. D. Pack, *Phys. Rev. B*, 1976, **13**, 5188-5192.
2. G. Kresse and J. Furthmüller, *Comput. Mater. Sci.*, 1996, **6**, 15-50.
3. J. P. Perdew, K. Burke and M. Ernzerhof, *Phys. Rev. Lett.*, 1996, **77**, 3865-3868.
4. J. Awaka, A. Takashima, K. Kataoka, N. Kijima, Y. Idemoto and J. Akimoto, *Chem. Lett.*, 2011, **40**, 60-62.
5. S. P. Ong, W. D. Richards, A. Jain, G. Hautier, M. Kocher, S. Cholia, D. Gunter, V. L. Chevrier, K. A. Persson and G. Ceder, *Comp Mater Sci*, 2013, **68**, 314-319.
6. L. J. Miara, S. P. Ong, Y. F. Mo, W. D. Richards, Y. Park, J. M. Lee, H. S. Lee and G. Ceder, *Chem. Mater.*, 2013, **25**, 3048-3055.
7. A. Jain, S. P. Ong, G. Hautier, W. Chen, W. D. Richards, S. Dacek, S. Cholia, D. Gunter, D. Skinner and G. Ceder, *APL Materials*, 2013, **1**, 011002.
8. K. A. Persson, B. Waldwick, P. Lazic and G. Ceder, *Phys. Rev. B*, 2012, **85**.
9. J. Speight, *Lange's Handbook of Chemistry, 70th Anniversary Edition*, McGraw-Hill Companies, Incorporated, 2004.
10. C. R. Mariappan, M. Gellert, C. Yada, F. Rosciano and B. Roling, *Electrochemistry Communications*, 2012, **14**, 25-28.
11. F. Tietz, T. Wegener, M. T. Gerhards, M. Giarola and G. Mariotto, *Solid State Ionics*, 2013, **230**, 77-82.
12. M. H. Brooker and J. B. Bates, *The Journal of Chemical Physics*, 1971, **54**, 4788-4796.